Pergamon

Tetrahedron 58 (2002) 8857–8861

TETRAHEDRON

# An important role of water in construction and destruction of the sheet structure in dipeptide aggregate

Motohiro Akazome,[a] Toshiaki Takahashi,[b] Ryo-ichi Sonobe[a] and Katsuyuki Ogura[a,*]

[a]*Department of Materials Technology, Faculty of Engineering, Chiba University, 1-33 Yayoicho, Inageku, Chiba 263-8522, Japan*
[b]*Graduate School of Science and Technology, Chiba University, 1-33 Yayoicho, Inageku, Chiba 263-8522, Japan*

Received 15 July 2002; accepted 19 August 2002

**Abstract**—Water molecules affect construction and destruction of inclusion crystals of a simple dipeptide (**1**). In the presence of water, the inclusion crystals, which have a water-buried dipeptide sheet structure, are smoothly constructed from amorphous solid of **1**. But, the sheet is thermally unstable than anhydrous one. 

## 1. Introduction

Water molecules are ubiquitous and play an essential role in constructing high-ordered supramolecular assembles of bioorganic substances such as proteins, carbohydrates, and nucleic acids.[1] In proteins, the internal water not only fills the structural cavities, but is necessary to stabilize the three-dimensional folding, especially α-helix.[2,3] This is achieved by hydrogen bonding to unsatisfied donor or acceptor sites or by mediating charges. During our investigation on the inclusion phenomena of (*R*)-arylglycyl-(*R*)-phenylglycine (**1**) crystals with an ether to form a 'parallel' mode structure or with an alcohol to form an 'antiparallel' mode structure (Fig. 1),[4–7] it was found that water promotes the crystallization of **1** to construct a new type of 'water-buried sheet' and give inclusion crystals. To data, sorptive inclusion of volatile guests with several organic host molecules via vapor contact have been reported,[8–10] but the ambiguous effect of water on the inclusion phenomena has had less attention.[11,12] Here, we wish to report the great role of water molecules not only in the formation of the inclusion crystals of **1**, but also in their thermal degradation.

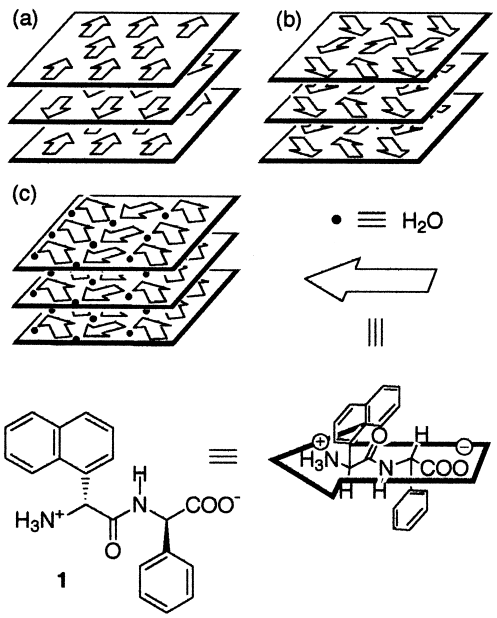


**Figure 1.** Schematic drawings of hydrogen-bonding sheets of **1** backbones. (a) Parallel mode. (b) Antiparallel mode. (c) Water-buried mode.

## 2. Results and discussion

Guest-free dipeptide **1** (an apohost) was prepared by evaporating a solution of **1** in methanol and dried over 2 h at 115°C. The powder X-ray diffraction (PXRD) pattern confirmed that it is practically amorphous. The contact of the apohost with the gaseous guest was carried out in a sealed vessel, in which the apohost of **1** was exposed to either an ether vapor or an ether–water vapor at ambient temperature for 4 d. Under anhydrous conditions, diethyl ether (**2**) vapor had no effect on formation of the inclusion crystals because the PXRD pattern remained unchanged (Fig. 2a), while 1,2-dimethoxyethane (DME; **3**) exhibited a partial effect on the construction of the inclusion crystals. On exposure of the apohost **1** with the vapor of **3**, the PXRD pattern (Fig. 2b) became resemblant to that of the cocrystallized **1**·**3** (vide infra), indicating that the inclusion crystals having a layer structure were constructed to a certain extent (the value of guest/host=0.38). By the single-crystal X-ray analysis of the cocrystallized **1**·**3**, a strong peak in the lower angle region of the PXRD pattern was

*Keywords*: inclusion compounds; peptides; hydrates; host–guest systems; crystal engineering.

* Corresponding author. Tel.: +81-43-290-3388; fax: +81-43-290-3402; e-mail: katsu@galaxy.tc.chiba-u.ac.jp

0040–4020/02/$ - see front matter 
PII: S0040-4020(02)01060-8

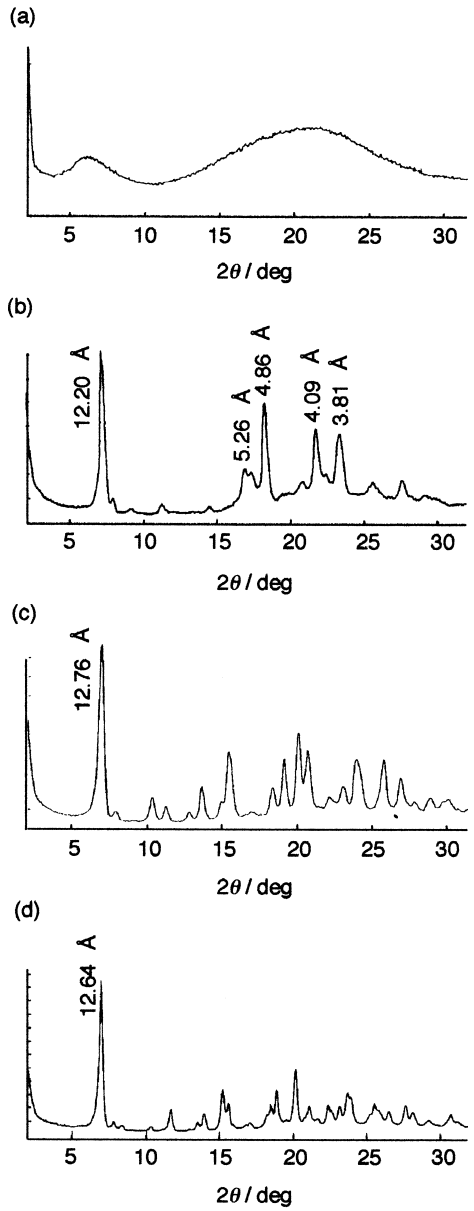


**Figure 2.** Powder X-ray diffraction patterns of apohost **1** exposed to the following gaseous guests for 4 days: (a) **2**; (b) **3**; (c) **2** and $H_2O$; (d) **3** and $H_2O$.

assigned as the layer distance between the (020) planes of dipeptide sheet structures. It should be noted that the coexistence of water vapor accelerates the formation of the inclusion crystals drastically. The crystals including **2** or **3** as a guest were smoothly produced to have the ratios of **1**–**2**–$H_2O$=1:0.81:0.93 or **1**–**3**–$H_2O$=1:0.60:0.78, respectively (Fig. 2c and d). The structures of the resulting inclusion crystals are the same as those obtained by cocrystallization of **1** and **2** (or **3**) in the presence of water. Since these crystals have the water-buried dipeptide sheets, it was indicated that the dipeptide sheet including internal water molecules can be formed more easily than the sheet that consists only of the dipeptide molecules.

The water-buried inclusion crystals with the ether were prepared by crystallization from a solution of **1** and the ether (more than 2 mol. equiv. to **1**) in aqueous methanol (MeOH–$H_2O$=3:1). The crystal structure of **1**·**3**·$H_2O$ is

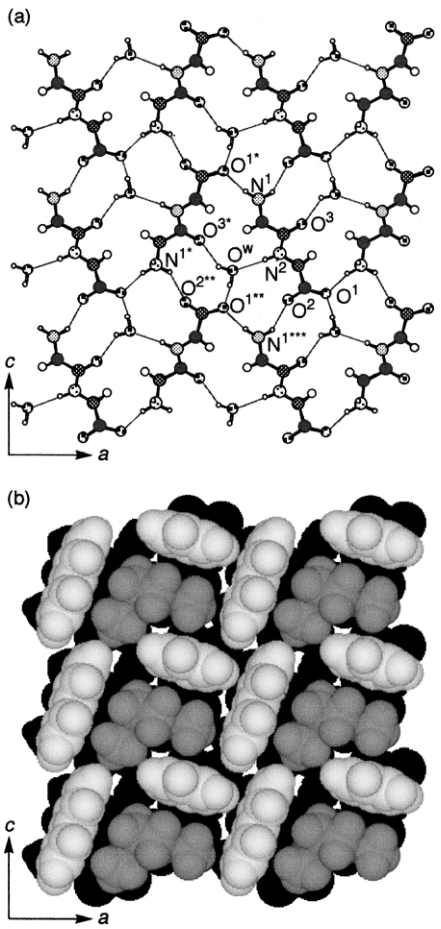


**Figure 3.** (a) The sheet structure of dipeptide backbones of the inclusion compound (**1**·**3**·$H_2O$) (the $a$–$c$ plane). The naphthyl and phenyl groups of **1** and **3** are omitted for clarity. (b) The space-filling model of packing in **1**·**3**·$H_2O$ (the $a$–$c$ plane). The naphthyl and phenyl groups of **1** and **3** are colored white and gray, respectively.

shown in Figs. 3 and 4. The salt formation between the amino and carboxyl groups of **1** contributes to the linkage of the dipeptide molecules ($N^1\cdots O^{1*}$ and $N^{1***}\cdots O^2$, 2.71 and 2.73 Å, respectively) to form a sheet structure along the $a$–$c$ axis (Fig. 3a). The dipeptides are arranged into a herring-bone motif by salt formation along the $a$ and $c$ axes. A water molecule ($O^W$) was effectively bridged by three hydrogen bonds between three dipeptides ($O^{3*}\cdots O^W$, $O^{1**}\cdots O^W$, and $N^{2}\cdots O^W$, 2.72, 2.72, and 2.83 Å, respectively) to fill the vacancy in the dipeptide sheet. Thus, we call this sheet structure a water-buried mode.

The inclusion cavity of **1**·**3**·$H_2O$ is shown in Fig. 3b. The naphthyl and phenyl groups of **1** stand perpendicular to the sheet to form an L-shaped cavity. This cage was surrounded by three naphthyl and two phenyl groups, which stacked at almost right angles in a T-shaped mode. T-shaped and slipped parallel modes of interaction between two molecules of benzene have comparable energies.[13]

Between the layer structures, the oxygen atoms of **3** anchored to the $^+NH_3$ of the dipeptide via hydrogen bonding. Distances of $O^{G1}\cdots N^1$ ($O^{G1}\cdots H^1$) and $O^{G2}\cdots N^1$ ($O^{G2}\cdots H^1$) are 2.82 (2.06) and 3.07 (2.49) Å, and the angles of $O^{G1}\cdots H–N^1$ and $O^{G2}\cdots H–N^1$ are 157° and 129°,

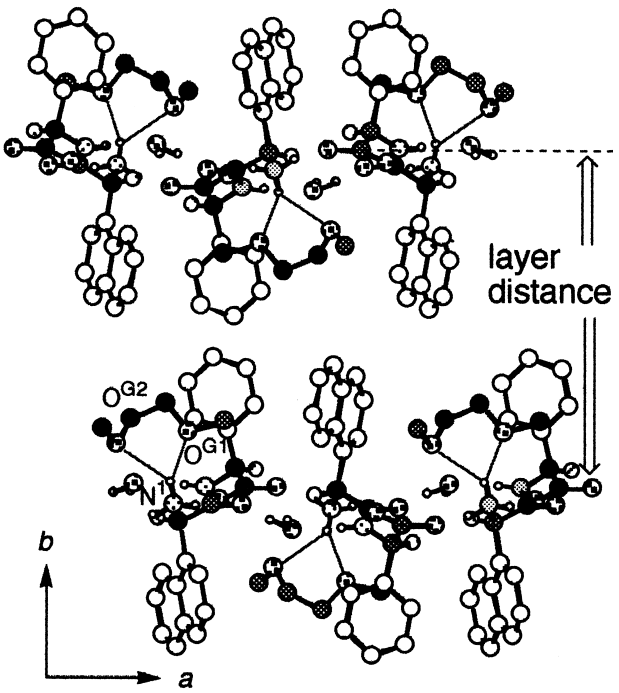


**Figure 4.** Layer structure of the inclusion compound of **1**·**3**·$H_2O$ (the $a-b$ plane). Dotted lines mean hydrogen bonds between $^+NH_3$ ($N^1$) of **1** and oxygen atoms ($O^{G1}$ and $O^{G2}$) of **3**. Hydrogen atoms of the naphthyl and phenyl groups of **1** and **3** are omitted for clarity. The naphthyl and phenyl groups of **1** are colored white.

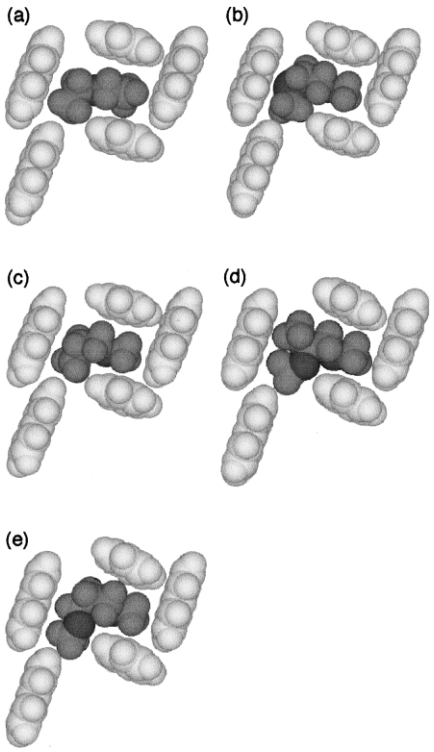


**Figure 5.** Comparison of L-shaped cavities for various guest molecules: (a) **1**·**2**·$H_2O$ (1:1:1), (b) **1**·**4**·$H_2O$ (1:1:1), (c) **1**·**5**·$H_2O$ (1:1:1), (d) **1**·(*S*)-**6**·$H_2O$ (1:1:1), (e) **1**·**7**·$H_2O$ (1:1:1). The naphthyl and phenyl groups of **1** and guest molecules are colored white and gray, respectively.

respectively. This three-center hydrogen bond would be comparable to that of anhydrous inclusion of **3**.[6]

In addition to **2** and **3**, ethers such as 1-methoxy-2-methylthioethane (**4**), 1-methoxypropane (**5**), 1,2-dimethoxypropane (**6**), 1,3-dimethoxypropane (**7**) formed the water-buried inclusion crystals, which are stable at ambient temperature in air. In these inclusion crystals, the arrangement of **1** molecules is similar to that of **1**·**3**·$H_2O$. The generality of L-shaped cavities is shown in Fig. 5. Interestingly, when the racemic compound **6** was used as a guest, only the (*S*)-enantiomer of **6** was stereoselectively included in the cavity.

In this L-shaped cavity, the size of the guest molecule would be restricted. In fact, tetrahydrofuran (**8**) did not give rise to the formation of water-buried inclusion crystals, but preferred inclusion crystals with the channel cavity without the incorporation of water molecules.[4] Other ethers such as 2-methoxypropane, 1-ethoxypropane, 1-methoxybutane, and 2,3-dimethoxybutane were mismatched to form the water-buried nor water-free inclusion crystals.

As reported in our previous papers, the water-free inclusion crystals with the ethers (**2**, **3** and **8**) could be obtained.[4–6] In these crystals, the dipeptide molecules were arranged in a parallel mode with a channel cavity, in which the ether molecules are accommodated. The water-free inclusion compound (**1**·**2**) is unstable. As soon as the inclusion crystals were taken off from the mother liquid, the transparent colorless crystals changed into an obscure white solid. In contrast, the inclusion compound (**1**·**3**) was stable at ambient temperature. Therefore, the thermal

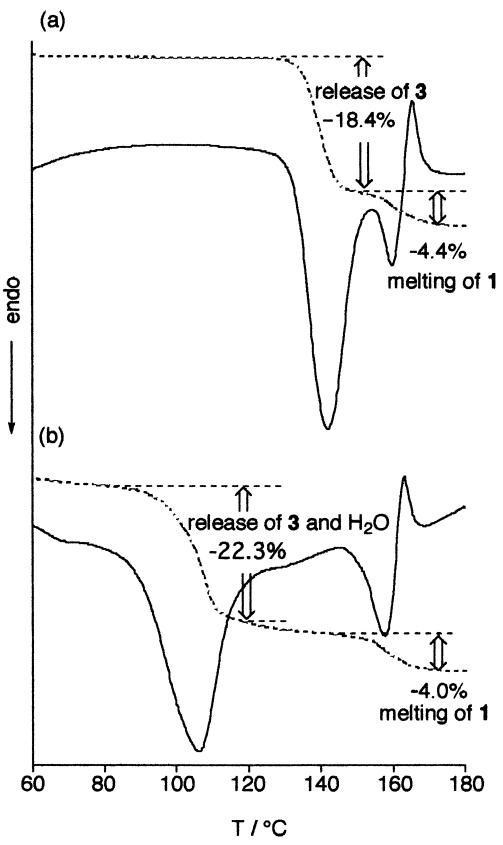


**Figure 6.** TG–DTA curves of the inclusion compounds of (a) **1**·**3** and (b) **1**·**3**·$H_2O$. TG and DTA curves are dashed and solid lines, respectively.

behavior of this inclusion compound was analyzed by TG–DTA (Fig. 6). The inclusion compound (**1**·**3**) released the guest (**3**) from the crystal lattice at 130–145°C to become an amorphous solid. The resulting dipeptide melted at 145–160°C and then changed to the corresponding diketopiperazine by the intramolecular dehydration (Fig. 6a). To our surprise, the water-buried inclusion compound (**1**·**3**·$H_2O$) lost both the guest (**3**) and the water at 85–120°C to become an amorphous solid (Fig. 6b). These facts suggested that **1**·**3** is more thermally stable than the water-buried compound (**1**·**3**·$H_2O$). This phenomenon can be rationalized in terms of enthalpy and entropy. The entropy loss in the formation of **1**·**3** is thought to be smaller than that in the formation of **1**·**3**·$H_2O$, because these inclusion compounds consist of two components and of three components, respectively. However, **1**·**3**·$H_2O$ would be advantageous in enthalpy because the water molecules function as an integral part of the sheet structure and their four accepting and donating points contribute to the hydrogen bonding in the sheet and, as a result, make their formation favorable in enthalpy. Generally speaking from the equation $\Delta G=\Delta H-T\Delta S$, the entropy term ($T\Delta S$) becomes significant at higher temperature. Therefore, three-component **1**·**3**·$H_2O$ decomposes more easily than **1**·**3**. It is emphasized that, at lower temperature such as room temperature, the water-buried sheet is smoothly constructed by the favorable contribution of the enthalpy term.

## 3. Conclusion

In summary, water molecules affect the nature of inclusion compounds of a simple dipeptide (**1**). The presence of water promoted the inclusion of guest molecules. It is noteworthy that the water-buried sheet was smoothly constructed from an amorphous solid of **1**, but the resulting inclusion compound (**1**·**3**·$H_2O$) decomposed easier at high temperature than the inclusion compound (**1**·**3**). We elucidated that water participates in the inclusion phenomenon and the folding structures of the dipeptide assembles as well as bioorganic substances.

## 4. Experimental

### 4.1. General experiments

The ratios of host–ether of the inclusion compounds were estimated by $^1$H NMR and TG–DTA. The amount of water was calculated by elemental analysis and TG–DTA. The ratios of host–guest–$H_2O$ were complementarily determined. Decomposition points were also determined by TG–DTA. PXRD patterns were obtained with a MAC Science MXP18 diffractometer using graphite-monochromated Cu Kα radiation (30 kV, 200 mA). The spectra were measured at room temperature between 2° and 50° in the $2\theta/\theta$-scan mode with steps of 0.01° in $2\theta$ and 4°/min. Diffraction data were presented in $d$ Å and relative reflecting intensities are in the parenthesis. Single-crystal X-ray analysis was performed on a Mac Science MXC18 four-circle diffractometer with graphite-monochromated Cu Kα ($\lambda$=1.541 78) radiation using the $2\theta-\omega$ scan technique, and the X-ray intensities were measured up to $2\theta$=140° at 298 K. The structures were solved by a direct method SIR 92 and refined by a computer program package; CRYSTAN-GM ver. 6.2.1 or maXus ver. 1.1 from MAC Science Co. Ltd.

### 4.2. Formation of inclusion compounds from amorphous 1 with gaseous guests

Amorphous (*R*)-(1-naphthyl)glycyl-(*R*)-phenylglycine (**1**)[7] was prepared by evaporating its methanolic solution and then being dried for 2 h at 115°C. Solid–gas experiments were carried out in a sealed vessel containing diethyl ether (2 mL) or water–diethyl ether (4 mL, 1:1 v/v) in the bottom. Amorphous **1** (67 mg, 0.2 mmol) was placed in a paper dish that was hung in the midair of the vessel and exposed to the vapor of diethyl ether or diethyl ether–water at an ambient temperature. After four days, these solids in the dish were analyzed (Fig. 2).

### 4.3. Preparation of hydrated inclusion compounds

To a solution of **1** (0.10 mmol) in 0.4 mL aqueous methanol (MeOH–$H_2O$=3:1) was added guest molecules (more than 2 mol. equiv.). The solution was allowed to stand at room temperature in a dry box. After several days, the precipitated crystals were collected by filtration, washed with chloroform (3 mL), and dried in vacuo to afford the inclusion compound.

**4.3.1. (*R*)-(1-Naphthyl)glycyl-(*R*)-phenylglycine·diethyl ether·$H_2O$ complex (1·2·$H_2O$).** A colorless solid; dec. 89.8°C (guest release); PXRD (Å ($I/I_0$)) 12.8 (1.00), 4.28 (0.34). Anal. Calcd for $C_{20}H_{18}N_2O_3\cdot1.00C_4H_{10}O\cdot1.00H_2O$: C, 67.59; H, 7.09; N, 6.57. Found: C, 67.28; H, 6.97; N, 6.58. $M$=426.51, orthorhombic, $P2_12_12_1$, $a$=11.712(3), $b$=25.600(6), $c$=7.836(2) Å, $V$=2349(1) Å$^3$, $Z$=4, $T$=298 K, $D_{calc}$=1.21 g cm$^{-3}$, 2780 reflections measured, 2567 independent, $R$=0.054 (1338 reflections with $I>3.00\sigma(I)$), $Rw$=0.062, 352 parameters, residual electron density 0.24/−0.20.

**4.3.2. (*R*)-(1-Naphthyl)glycyl-(*R*)-phenylglycine·1,2-dimethoxyethane·$H_2O$ complex (1·3·$H_2O$).** Colorless plate; dec. 93.3°C (guest release); PXRD (Å ($I/I_0$)) 12.6 (1.00), 6.31 (0.06), 4.20 (0.20). Anal. Calcd for $C_{20}H_{18}N_2O_3\cdot1.00C_4H_{10}O_2\cdot1.00H_2O$: C, 65.14; H, 6.83; N, 6.33. Found: C, 64.91; H, 6.86; N, 6.23. $M$=442.50, orthorhombic, $P2_12_12_1$, $a$=11.683(3), $b$=25.242(5), $c$=7.942(2) Å, $V$=2342.0(9) Å$^3$, $Z$=4, $T$=298 K, $D_{calc}$=1.25 g cm$^{-3}$, 2656 reflections measured, 2458 independent, $R$=0.0475 (2067 reflections with $I>3.00\sigma(I)$), $Rw$=0.0569, 367 parameters, residual electron density 0.30/−0.22.

**4.3.3. (*R*)-(1-Naphthyl)glycyl-(*R*)-phenylglycifle·1-methoxy-2-methylthioethane·$H_2O$ complex (1·4·$H_2O$).** A pale yellow solid; dec. 74.8°C (guest release); PXRD (Å ($I/I_0$)) 12.58 (1.00), 4.44 (0.13), 4.18 (0.19), 3.70 (0.08), 3.14 (0.07). Anal. Calcd for $C_{20}H_{18}N_2O_3\cdot1.00C_4H_{10}OS\cdot1.00H_2O$: C, 62.86; H, 6.59; N, 6.11. Found: C, 62.74; H, 6.47; N, 6.20. $M$=458.58, orthorhombic, $P2_12_12_1$, $a$=11.867(3), $b$=25.100(6), $c$=7.955(3) Å, $V$=2369(1) Å$^3$, $Z$=4, $T$=298 K, $D_{calc}$=1.29 g cm$^{-3}$, 2697 reflections measured, 2257

independent, $R$=0.066 (2121 reflections with $I>1.00\sigma(I)$), $Rw$=0.077, 349 parameters, residual electron density 0.34/−0.41.

**4.3.4. (*R*)-(1-Naphthyl)glycyl-(*R*)-phenylglycine·1-methoxypropane·$H_2O$ complex (1·5·$H_2O$).** A colorless plate; dec. 85.7°C (guest release); PXRD (Å ($I/I_0$)) 12.65 (1.00), 5.70 (0.07), 4.21 (0.32), 3.16 (0.08), 2.73 (0.04). $M$=426.51, orthorhombic, $P2_12_12_1$, $a$=11.706(3), $b$=25.321(7), $c$=7.844(2) Å, $V$=2325(1) Å$^3$, $Z$=4, $T$=298 K, $D_{calc}$=1.22 g cm$^{-3}$, 2639 reflections measured, 2206 independent, $R$=0.061 (1470 reflections with $I>1.50\sigma(I)$), $Rw$=0.056, 313 parameters, residual electron density 0.19/−0.18.

**4.3.5. (*R*)-(1-Naphthyl)glycyl-(*R*)-phenylglycine·1,2-dimethoxypropane·$H_2O$ complex (1·6·$H_2O$).** A colorless plate; dec. 90.1°C (guest release); PXRD (Å ($I/I_0$)) 12.6 (1.00), 6.28 (0.10), 4.48 (0.07), 4.18 (0.65), 3.69 (0.05), 3.13 (0.09), 3.03 (0.04). Anal. Calcd for $C_{20}H_{18}Na_2O_3{\cdot}1.03C_5H_{12}O_2{\cdot}1.04H_2O$: C, 65.61; H, 7.10; N, 6.08. Found: C, 65.24; H, 6.94; N, 6.24. $M$=456.53, orthorhombic, $P2_12_12_1$, $a$=12.179(3), $b$=25.048(5), $c$=7.839(2) Å, $V$=2391(1) Å$^3$, $Z$=4, $T$=298 K, $D_{calc}$=1.31 g cm$^{-3}$, 2711 reflections measured, 2603 independent, $R$=0.045 (1871 reflections with $I>3.00\sigma(I)$), $Rw$=0.049, 393 parameters, residual electron density 0.19/−0.18.

**4.3.6. (*R*)-(1-Naphthyl)glycyl-(*R*)-phenylglycine·1,3-dimethoxypropane·$H_2O$ complex (1·7·$H_2O$).** A colorless plate; dec. 93.9°C (guest release); PXRD (Å ($I/I_0$)) 12.4 (1.00), 6.21 (0.37), 4.15 (0.52). Anal. Calcd for $C_{20}H_{18}N_2O_3{\cdot}1.00C_5H_{12}O_2{\cdot}0.98H_2O$: C, 65.82; H, 7.06; N, 6.14. Found: C, 66.09; H, 6.78; N, 6.24. $M$=456.53, orthorhombic, $P2_12_12_1$, $a$=11.980(3), $b$=25.028(6), $c$=7.967(2) Å, $V$=2389(1) Å$^3$, $Z$=4, $T$=298 K, $D_{calc}$=1.27 g cm$^{-3}$, 2719 reflections measured, 2435 independent, $R$=0.046 (2213 reflections with $I>3.00\sigma(I)$), $Rw$=0.053, 390 parameters, residual electron density 0.26/−0.36.

Crystallographic data (excluding structure factors) for the structures reported in this paper have been deposited with the Cambridge Crystallographic Data Centre as supplementary publication nos. CCDC-185322–185327. Copies of the data can be obtained free of charge on application to CCDC, 12 Union Road, Cambridge CB21EZ, UK (fax: +44-1223-336-033; email: deposit@ccdc.cam.ac.uk).

## References


1. Jeffrey, G. A.; Saenger, W. *Hydrogen Bonding in Biological Structures*; Springer: New York, 1991.
2. Sundaralingam, M.; Sekharudu, Y. C. *Science* **1989**, *244*, 1333–1337.
3. Parthasarathy, R.; Chaturvedi, S.; Go, K. *Proc. Natl Acad. Sci. USA* **1990**, *87*, 871–875.
4. Akazome, M.; Sumikawa, A.; Sonobe, R.; Ogura, K. *Chem. Lett.* **1996**, 995–996.
5. Akazome, M.; Yanagita, Y.; Sonobe, R.; Ogura, K. *Bull. Chem. Soc. Jpn* **1997**, *70*, 2823–2827.
6. Akazome, M.; Takahashi, T.; Sonobe, R.; Ogura, K. *Supramol. Chem.* **2001**, *13*, 109–136.
7. Akazome, M.; Takahashi, T.; Ogura, K. *J. Org. Chem.* **1999**, *64*, 2293–2300.
8. Dewa, T.; Endo, K.; Aoyama, Y. *J. Am. Chem. Soc.* **1998**, *120*, 8933–8940.
9. Scott, J. L. *J. Chem. Soc., Perkin Trans. 2* **1995**, 495–502.
10. Weber, E.; Wimmer, C.; Llamas-Saiz, A. L.; Foces-Foces, C. *J. Chem. Soc., Chem. Commun.* **1992**, 734–735.
11. Caira, M. R.; Nassinbeni, L. R.; Scott, J. L. *J. Chem. Soc., Perkin Trans. 2* **1994**, 1403–1405.
12. Hishikawa, Y.; Sada, K.; Miyata, M. *J. Chem. Res. (S)* **1998**, 738–739.
13. Tsuzuki, S.; Honda, K.; Uchimura, T.; Mikami, M.; Tanabe, K. *J. Am. Chem. Soc.* **2002**, *124*, 104–112.